PHYSICAL REVIEW E **83**, 060501(R) (2011)

Equilibration of concentrated hard-sphere fluids

Gabriel Pérez-Ángel,[1] Luis Enrique Sánchez-Díaz,[2] Pedro E. Ramírez-González,[2] Rigoberto Juárez-Maldonado,[2,3] Alejandro Vizcarra-Rendón,[3] and Magdaleno Medina-Noyola[2]

[1]*Departamento de Física Aplicada, Centro de Investigación y de Estudios Avanzados del Instituto Politécnico Nacional, Unidad Mérida, Apartado Postal 73 Cordemex, 97310, Mérida, Yucatán, Mexico*

[2]*Instituto de Física "Manuel Sandoval Vallarta," Universidad Autónoma de San Luis Potosí, Álvaro Obregón 64, 78000 San Luis Potosí, San Luis Potosí, Mexico*

[3]*Unidad Académica de Física, Universidad Autónoma de Zacatecas, Paseo la Bufa y Calzada Solidaridad, 98600, Zacatecas, Zacatecas, Mexico*

(Received 2 November 2010; revised manuscript received 31 January 2011; published 23 June 2011)

We report a systematic molecular dynamics study of the isochoric equilibration of hard-sphere fluids in their metastable regime close to the glass transition. The thermalization process starts with the system prepared in a nonequilibrium state with the desired final volume fraction ϕ for which we can obtain a well-defined *nonequilibrium* static structure factor $S_0(k;\phi)$. The evolution of the α-relaxation time $\tau_\alpha(k)$ and long-time self-diffusion coefficient D_L as a function of the evolution time t_w is then monitored for an array of volume fractions. For a given waiting time the plot of $\tau_\alpha(k;\phi,t_w)$ as a function of ϕ exhibits two regimes corresponding to samples that have fully equilibrated within this waiting time [$\phi \leqslant \phi^{(c)}(t_w)$] and to samples for which equilibration is not yet complete [$\phi \geqslant \phi^{(c)}(t_w)$]. The crossover volume fraction $\phi^{(c)}(t_w)$ increases with t_w but seems to saturate to a value $\phi^{(a)} \equiv \phi^{(c)}(t_w \to \infty) \approx 0.582$. We also find that the waiting time $t_w^{\rm eq}(\phi)$ required to equilibrate a system grows faster than the corresponding equilibrium relaxation time, $t_w^{\rm eq}(\phi) \approx 0.27[\tau_\alpha^{\rm eq}(k;\phi)]^{1.43}$, and that both characteristic times increase strongly as ϕ approaches $\phi^{(a)}$, thus suggesting that the measurement of *equilibrium* properties at and above $\phi^{(a)}$ is experimentally impossible.

DOI: 10.1103/PhysRevE.83.060501 PACS number(s): 64.70.pm, 05.40.−a, 64.70.pv, 64.70.Q−

Above a certain size polydispersity, real and simulated hard-sphere liquids fail to crystalize for volume fractions ϕ beyond the freezing point $\phi^{(f)} = 0.494$ of the monodisperse system [1–4]. As ϕ increases, the viscosity increases enormously, and the metastable liquid eventually becomes an amorphous solid. Mode-coupling theory (MCT) [5] predicts a transition from metastable fluid to ideal nonergodic states, characterized by the vanishing of the long-time self-diffusion coefficient D_L and the divergence of both the α-relaxation time τ_α and the viscosity η. For the hard-sphere fluid the phenomenology predicted by MCT at $\phi^{(a)} \approx 0.52$ has been essentially confirmed by the experimental observations in hard-sphere colloidal suspensions at $\phi^{(a)}_{\rm exp} \approx 0.58$ [6,7], although a number of intrinsic experimental uncertainties render the precise determination of $\phi^{(a)}_{\rm exp}$ a topic of recurrent scientific discussion [4,6–10].

The recent work of Brambilla *et al.* [9,10], however, seems to put the very experimental relevance of the divergent scenario predicted by MCT under severe questioning. By fitting their dynamic light-scattering data with the asymptotic expression $\tau_\alpha(\phi) \sim (\phi^{(a)} - \phi)^{-\gamma}$, traditionally associated with MCT, these authors determined $\phi^{(a)}$ to be $\phi^{(a)} = 0.590 \pm 0.005$. If the ideal MCT picture were to be observed in their experiments, the measured $\tau_\alpha(\phi)$ should be infinite for $\phi > \phi^{(a)}$. Instead, for the volume fraction range $\phi^{(a)} < \phi \lesssim 0.6$, they report large but finite relaxation times, determined through an extremely careful experimental procedure designed to deal with artifacts caused, for example, by sample heating or sedimentation, which allowed them to accurately monitor the equilibration process of their samples [10]. Thus, the most immediate interpretation is that these measurements involve macroscopic states in which the system, instead of falling out of equilibrium, remains ergodic but enters a new dynamical regime where τ_α increases with volume fraction according to a different functional form, namely, $\tau_\alpha(\phi) \sim \tau_\infty \exp[A(\phi_0 - \phi)^{-\delta}]$. This functional form had been proposed by at least two prior theoretical works specifically formulated for equilibrated, very dense, hard-sphere suspensions [11,12].

This interpretation, however, rests on the assumption that all measurements reporting an apparent stationary behavior indeed involve fully equilibrated systems. Recent molecular dynamics simulations [13,14], however, suggest that this assumption should not be taken for granted without further discussion. For example, according to Ref. [13], the relaxation time $\tau_{\rm hetero}$ of dynamic heterogeneities may grow like $\tau_{\rm hetero} \sim \tau_\alpha^{1.5}$ as the glass transition is approached. Thus, if one has to wait until "slow" regions become "fast" regions and vice versa, one possibility that cannot be ruled out is that when the *equilibrium* relaxation time $\tau_\alpha^{\rm eq}(\phi)$ indeed diverges, the system will require a similarly divergent *equilibration* time $t_w^{\rm eq}(\phi)$, thus blurring even the most accurate observation. Motivated in part by these considerations, here we *intentionally* study the effects on $\tau_\alpha(\phi)$ of the *incomplete* equilibration of concentrated hard-sphere systems close to the glass transition by means of systematic computer simulations, in which some of the intrinsic uncertainties of the experimental samples will be absent.

As in Ref. [14], the basic simulation experiment consists of monitoring the irreversible evolution of a hard-sphere system initially prepared at a nonequilibrium state characterized by a prescribed volume fraction ϕ and by a well-defined nonequilibrium static structure factor $S_0(k;\phi)$. The irreversible evolution to equilibrium is then described in terms of the time-evolving nonequilibrium static structure factor $S_{t_w}(k;\phi)$ and self-intermediate scattering function (self-ISF) $F_S(k,\tau,t_w)$, where t_w is the *waiting* ("evolution") time after the system was prepared. The naturally expected long-t_w asymptotic

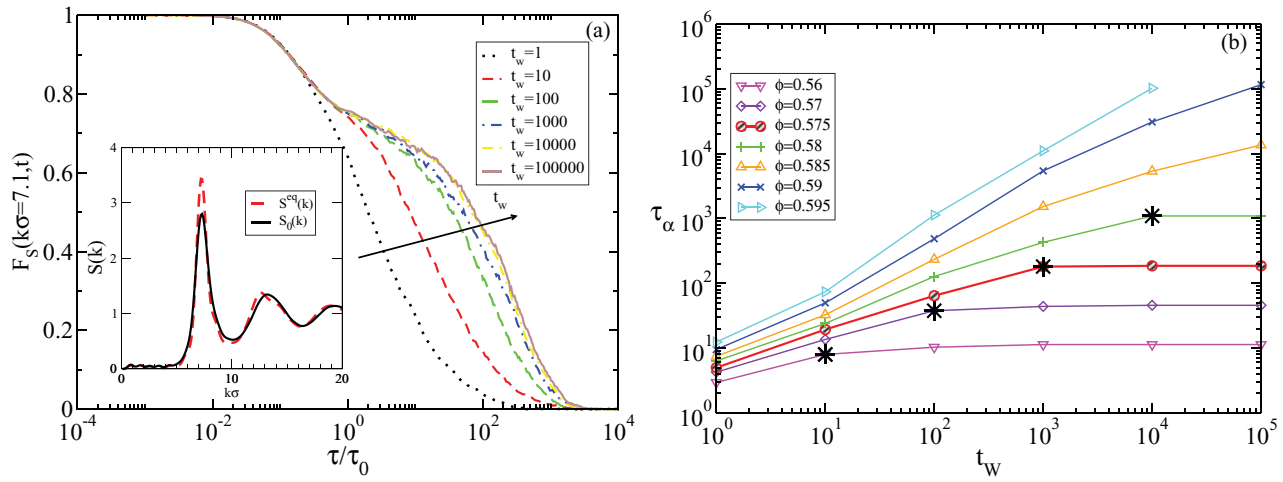

FIG. 1. (Color online) (a) Self-intermediate scattering function $F_S(k,\tau;t_w)$ of a polydisperse hard-sphere system ($s = 0.0866$) evaluated at $k = 7.1$ at volume fraction $\phi = 0.575$ as a function of the correlation time τ for waiting times $t_w = 10^0, 10^1, \ldots, 10^5$. The inset in (a) shows the corresponding $S_0(k;\phi)$ (solid line) and $S^{eq}(k;\phi)$ (dashed line). (b) Simulation data of the α-relaxation time $\tau_\alpha(k;\phi,t_w)$ as a function of t_w at fixed volume fraction. The asterisks highlight the points $(t_w^{eq}(\phi),\tau_\alpha^{eq}(k;\phi))$.

limit of these properties is, of course, the *equilibrium* static structure factor $S^{eq}(k;\phi)$ and self-ISF $F_S^{eq}(k,\tau)$. Our interest is to determine the volume fractions for which equilibrium is reached within a given waiting time t_w.

We use event-driven molecular dynamics to simulate the evolution of $N = 1000$ particles in a volume V, with particle diameters σ evenly distributed between $\overline{\sigma}(1 - w/2)$ and $\overline{\sigma}(1 + w/2)$, with $\overline{\sigma}$ being the mean diameter. We consider the case $w = 0.3$, corresponding to a polydispersity $s_\sigma = w/\sqrt{12} = 0.0866$. According to the results reported in [3], at this polydispersity the system shows no evidence of crystallization for any volume fraction $\phi = (\pi/6)n\overline{\sigma^3}$, where $\overline{\sigma^3}$ is the third moment of the size distribution and n is the total number density $n \equiv N/V$. All the particles are assumed to have the same mass M. The length, mass, and time units employed are $\overline{\sigma}$, M, and $\overline{\sigma}\sqrt{M/k_BT}$, respectively.

To produce the initial configurations, we used soft-particle molecular dynamics to simulate the evolution of a set of initially overlapping, randomly placed particles, with the correct distribution of diameters, interacting through a short-ranged repulsive soft (but increasingly harder) interaction and in the presence of strong dissipation. For ϕ below the random close-packing limit, this system evolves rapidly into a disordered configuration with no overlaps. These nonthermalized hard-sphere configurations are then given random velocities generated by a Maxwell-Boltzmann distribution, with k_BT set as the energy unit. These configurations are then used as the starting configurations for the event-driven simulation of the hard sphere (HS) equilibration process.

The simulations were carried for an array of values of ϕ between 0.480 and 0.595. For each such volume fraction we used waiting times from 1 to 10^5 in powers of 10. The sequence of configurations obtained is employed to generate the self-ISF $F_S(k,\tau,t_w) \equiv (1/N)\langle\sum_{i=1}^N \exp\{i\mathbf{k}\cdot[\mathbf{r}_i(t_w+\tau)-\mathbf{r}_i(t_w)]\}\rangle$ and the mean square displacement $\langle[\Delta\mathbf{r}(\tau;t_w)]^2\rangle \equiv (1/N)\langle\sum_{i=1}^N[\mathbf{r}_i(t_w+\tau)-\mathbf{r}_i(t_w)]^2\rangle$, where $\mathbf{r}_i(t)$ is the position of the ith particle at time t, $\tau \equiv (t - t_w)$ is the *correlation* time, and the angle brackets indicate averaging over (at least) 20 independent realizations. $F_S(k,\tau;t_w)$ is evaluated at $k = 7.1$, close to the main peak of $S^{eq}(k;\phi)$ for all the values of ϕ considered. The α-relaxation time $\tau_\alpha(k;\phi,t_w)$ is defined by the condition $F_S(k,\tau_\alpha,t_w) = 1/e$, and the long-time self-diffusion coefficient D_L is defined by $D_L(\phi;t_w) \equiv \lim_{\tau\to\infty}\langle[\Delta\mathbf{r}(\tau;t_w)]^2\rangle/6\tau$.

Let us illustrate the results of this procedure for one specific volume fraction, namely, $\phi = 0.575$. In Fig. 1(a) we present the simulation results for $F_S(k,\tau;t_w)$ evaluated at $k = 7.1$ as a function of the correlation time τ for the sequence of waiting times $t_w = 10^0, 10^1, \ldots, 10^5$. This sequence exhibits the increasing slowing down of the dynamics as the system approaches its equilibrium state and illustrates the fact that $F_S(k,\tau;t_w)$ saturates to its equilibrium value $F_S^{eq}(k,\tau)$ after a certain *equilibration waiting time* $t_w^{eq}(\phi)$. For example, from the illustrative data in Fig. 1 we find that $t_w^{eq}(\phi = 0.575) \approx 10^4$. A similar evolution and saturation is observed in the static structure factor $S_{t_w}(k;\phi)$, which exhibits, as expected, a large increase at the first diffraction peak. The inset in Fig. 1(a) presents the initial static structure factor $S_0(k;\phi) \equiv S_{t_w=0}(k;\phi)$ and its final equilibrium value $S^{eq}(k;\phi)$. From the data for $F_S(k,\tau;t_w)$ in Fig. 1 we can determine the α-relaxation time $\tau_\alpha(k;\phi,t_w)$ as a function of t_w. The results indicate that the α-relaxation time $\tau_\alpha(k;\phi = 0.575,t_w)$ saturates approximately to its equilibrium value $\tau_\alpha^{eq}(k;\phi = 0.575) \approx 2 \times 10^2$ within the equilibration waiting time $t_w^{eq}(\phi = 0.575) \approx 10^4$.

Figure 1(b) plots the dependence of the α-relaxation time $\tau_\alpha(k;\phi,t_w)$ as a function of waiting time t_w for fixed volume fraction ϕ. These plots confirm that beyond an equilibration waiting time $t_w^{eq}(\phi)$, the α-relaxation time $\tau_\alpha(k;\phi)$ saturates approximately to its equilibrium value $\tau_\alpha^{eq}(k;\phi)$. To emphasize these concepts, we have highlighted the points $(t_w^{eq}(\phi),\tau_\alpha^{eq}(k;\phi))$ in Fig. 1(b). In fact, we notice that the highlighted points $(t_w^{eq}(\phi),\tau_\alpha^{eq}(k;\phi))$ obey the approximate relation $t_w^{eq}(\phi) \approx 0.27[\tau_\alpha^{eq}(k;\phi)]^{1.43}$, suggesting that the waiting time $t_w^{eq}(\phi)$ required to equilibrate a system is always longer than the corresponding equilibrium relaxation time $\tau_\alpha^{eq}(k;\phi)$ and that both characteristic times increase strongly with ϕ.

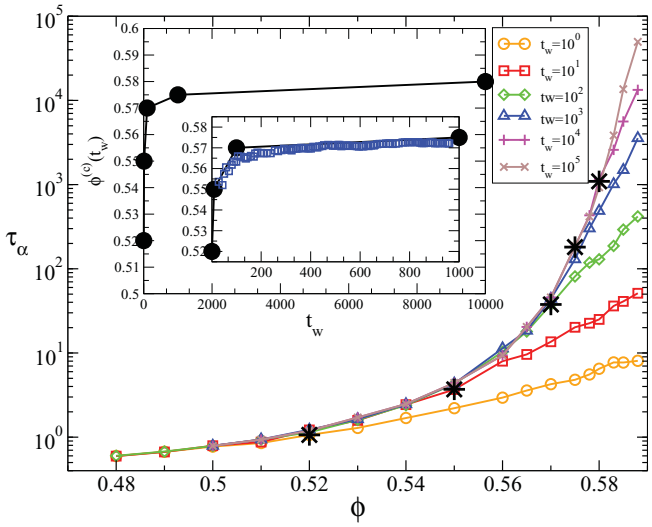

FIG. 2. (Color online) The same simulation data of the α-relaxation time $\tau_\alpha(k;\phi,t_w)$ as in Fig. 1, but now displayed as a function of volume fraction ϕ at fixed waiting time t_w. The asterisks indicate, in this case, the crossover volume fraction $\phi^{(c)}(t_w)$ at the various waiting times. The circles in the inset display the evolution of $\phi^{(c)}(t_w)$ with waiting time, and the squares are the corresponding results in Fig. 5(a) of Ref. [14].

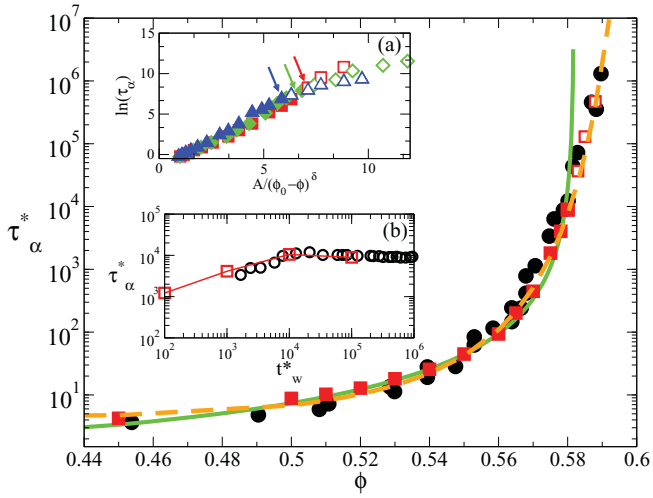

FIG. 3. (Color online) Volume fraction dependence of the scaled α-relaxation time $\tau^*(k;\phi,t_w) \equiv k^2 D^0 \tau_\alpha(k;\phi,t_w)$. The solid (empty) squares denote simulation data of fully equilibrated (insufficiently equilibrated) systems. The solid line represents the predictions of the SCGLE theory. The dashed line is the fit with $\tau_\alpha(\phi) = \tau_\infty \exp[A(\phi_0 - \phi)^{-\delta}]$. The solid circles correspond to the experimental results of Fig. 13 of Ref. [10]. Inset (a) plots $\ln[\tau_\alpha(k;\phi,t_w)]$ as a function of $A(\phi_0-\phi)^{-\delta}$ for $t_w = 10^5$ (squares), 10^4 (diamonds), and 10^3 (triangles), with the arrows pointing at the corresponding crossover volume fraction $\phi^{(c)}(t_w)$. Inset (b) compares our simulation results (empty squares with line) for $\tau^*(k;\phi,t_w)$ vs $t^*_w \equiv k^2 D^0 t_w$ for $\phi = 0.58$ with the experimental data of Fig. 6 of Ref. [10] (empty circles) at $\phi^{\rm exp} = 0.5876$.

Just like Hermes and Dijkstra [14] did with the pressure (see their Fig. 1), let us display our data for $\tau_\alpha(k;\phi,t_w)$ of Fig. 1(b) in a complementary manner, namely, as a function of volume fraction for fixed waiting time t_w, and this is done in Fig. 2. The first feature to notice in each of the corresponding curves is that one can distinguish two regimes in volume fraction, namely, the low-ϕ (equilibrated) regime and the high-ϕ (nonequilibrated) regime, separated by a crossover volume fraction $\phi^{(c)}(t_w)$. Focusing, for example, on the results corresponding to $t_w = 10^3$, we notice that $\phi^{(c)}(t_w = 10^3) \approx 0.57$. In Fig. 2 we have highlighted the crossover points $(\phi^{(c)}(t_w), \tau_\alpha^{\rm eq}(k;\phi))$. We observe that the resulting crossover volume fraction $\phi^{(c)}(t_w)$ first increases rather fast with t_w but then slows down considerably, suggesting a saturation to a value slightly larger than 0.58, as indicated in the inset of Fig. 2, which also include the results for $\phi^{(c)}(t_w)$ determined by Hermes and Dijkstra [14] from the pressure, denoted by η_g in their Fig. 5(a). The exact limit $\phi^{(c)}(t_w \to \infty)$, however, will hardly be determined by even more powerful simulations, and from a theoretical point of view a nonequilibrium approach is clearly required.

One of the main products of the simulation results just presented is the determination of the volume fraction dependence of the *equilibrium* α-relaxation time $\tau_\alpha^{\rm eq}(k;\phi)$. Clearly, our simulation experiment can determine this property only within the window $0 \leqslant \phi \leqslant \phi^{(c)}(t_w^{\rm max})$, where $t_w^{\rm max}$ is the maximum waiting time achieved in the simulation experiment. In our case, $t_w^{\rm max} = 10^5$, yielding $\phi^{(c)}(t_w^{\rm max}) \approx 0.58$. These results, scaled with $\tau_{\alpha,0}(k;\phi) \equiv 1/k^2 D^0$, with $D^0 = \sqrt{\pi}/16\phi$ (see below), are plotted in Fig. 3 as solid squares. For $\phi \geqslant 0.58$ the t_w-dependent α-relaxation time $\tau_\alpha(k;\phi,t_w)$ did not saturate to its equilibrium value within the total duration of the present simulation experiment. These results are also plotted in Fig. 3 as empty squares to denote insufficient equilibration. Thus, only the data in the solid squares are meaningful when comparing with the predictions of *equilibrium* theories such as MCT or the more recently developed self-consistent generalized Langevin equation (SCGLE) theory [15].

MCT and the SCGLE theory provide similar answers regarding the asymptotic divergence of the relaxation times. We consider, however, that there is no need to appeal to asymptotic expressions, which have a more restricted range of validity, when one has easy access to the full numerical solution of the corresponding theory, as we do for the SCGLE theory of colloid dynamics. As we have recently discovered [16], the latter theory also describes the long-time dynamics of atomic systems provided the solvent short-time self-diffusion coefficient D^0 is replaced by the kinetic-theory self-diffusion coefficient, given by $D^0 = \sqrt{\pi}/16\phi[\sigma\sqrt{k_B T/M}]$ [17,18]. In Fig. 3 we compare the simulated equilibrium data for $\tau^*(k;\phi,t_w) \equiv k^2 D^0 \tau_\alpha(k;\phi,t_w)$ ($\phi \leqslant 0.58$) with the predictions of the SCGLE theory [Eqs. (1), (2), and (5)–(8) of Ref [15], with $k_c = 8.48$ adjusted to fine-tune the comparison with these equilibrium data]. According to this fit, $\tau_\alpha^{\rm eq}(k;\phi)$ would diverge at $\phi^{(a)} \approx 0.582$.

There is, of course, no reason to include the nonequilibrated data of Fig. 3 in this comparison. As a mere fitting exercise, however, we notice that the full set including these nonequilibrated data can be fitted by the expression $\tau_\alpha(\phi) = \tau_\infty \exp[A(\phi_0 - \phi)^{-\delta}]$, thus finding $A = 0.02$, $\delta = 1.921$, $\tau_\infty = 0.21$, and $\phi_0 = 0.6235$ (dashed line in Fig. 3). Amazingly enough, we find that this functional form provides

a reasonable fit also for the shorter waiting times $t_w = 10^4$ and 10^3 using the same values for δ, C, and τ_∞, but with $\phi_0 = 0.631$ and 0.635, respectively, as illustrated in inset (a) of Fig. 3.

In order to relate our simulation results with the experimental observations of Refs. [9,10], in inset (b) of Fig. 3 we compare the experimental equilibration data of Fig. 6 of Ref. [10] for the sample labeled $\phi^{\rm exp} = 0.5876$, with the simulation data corresponding to $\phi = 0.58$ in Fig. 1(b) above. The excellent agreement between the simulated and the experimental equilibration data suggests that the difference in the value of ϕ and $\phi^{\rm exp}$ could be explained by the intrinsic uncertainties discussed in Ref. [10] regarding the determination of the volume fraction of the system.

Assuming that this is the case, we can directly compare our MD simulation results in Fig. 3 for $\tau_\alpha^{\rm eq}(k;\phi)/\tau_{\alpha,0}^{\rm eq}(k;\phi)$ with the experimental data in Fig. 13 of Ref. [10], provided that we assume a constant ratio $\phi/\phi^{\rm exp} = 0.58/0.5876 = 0.987$. The dark circles in Fig. 3 are precisely those experimental data as a function of the experimental volume fraction reduced by a factor 0.985 to approximately account for the referred uncertainties. In addition, as a simple manner to treat hydrodynamic interactions [19], we have to take into account that the role of the parameter D^0 is played, in the experimental data, by the short-time self-diffusion coefficient $D_S(\phi)$, given approximately by $D_S(\phi)/D_S(\phi = 0) = (1-\phi)/(1+1.5\phi)$ [20]. The resulting comparison in Fig. 3 suggests a completely similar phenomenology, although it is quite clear only in the case of our simulation data that the departure of $\tau_\alpha(k;\phi,t_w = 10^5)$ from the equilibrium curve predicted by the SCGLE theory near $\phi^{(a)}$ is due to the insufficient equilibration of the system within the maximum waiting time $t_w^{\rm max} = 10^5$ of our simulation experiment.

The results just presented suggest, however, that any simulation aimed at determining the *equilibrium* value of dynamic order parameters such as $\tau_\alpha(k;\phi,t_w)$ and $D_L(\phi;t_w)$ near the dynamic arrest transition is bound to be limited by the duration of the simulation experiment, represented by the maximum waiting time t_w involved. This limits the determination of these equilibrium values to the window of volume fractions $0 \leqslant \phi \leqslant \phi^{(c)}(t_w^{\rm max})$. For $\phi \geqslant \phi^{(c)}(t_w^{\rm max})$, the simulation results will be reporting the properties of an insufficiently equilibrated system. The results presented here indicate that if we want to enlarge this window, we would have to go to exponentially longer waiting times, which is bound sooner or later to become a lost battle. There is, of course, no obvious reason to believe that a different situation will prevail in experimental samples.

Let us finally notice that the expression $\tau_\alpha(\phi) = \tau_\infty \exp[A(\phi_0 - \phi)^{-\delta}]$ gives a reasonable fit for our nonequilibrium data, even at early stages in the waiting time t_w. Thus, in the present case it is clear that the dynamical regime described by this functional actually involves the lack of equilibration of the system, whose correct analysis must then be made in the framework of a nonequilibrium theory. It is pertinent to mention that our original motivation to carry out the present simulations was precisely the need to generate reliable data of incompletely equilibrated systems that will serve as a reference to test the recently developed nonequilibrium extension [21] of the SCGLE theory.

This work was supported by the Consejo Nacional de Ciencia y Tecnología (CONACYT, México), through Grants No. 84076 and No. CB-2006-C01-60064, and by Fondo Mixto CONACYT-SLP through Grant No. FMSLP-2008-C02-107543.

[1] B. J. Alder and T. E. Wainwright, J. Chem. Phys. **27**, 1208 (1957).
[2] P. N. Pusey and W. van Megen, Nature (London) **320**, 340 (1986).
[3] E. Zaccarelli *et al.*, Phys. Rev. Lett. **103**, 135704 (2009).
[4] P. N. Pusey and W. van Megen, Phys. Rev. Lett. **59**, 2083 (1987).
[5] W. Götze, in *Liquids, Freezing and the Glass Transition*, edited by J. P. Hansen, D. Levesque, and J. Zinn-Justin (North-Holland, Amsterdam, 1991).
[6] W. van Megen and P. N. Pusey, Phys. Rev. A **43**, 5429 (1991).
[7] W. van Megen, T. C. Mortensen, S. R. Williams, and J. Muller, Phys. Rev. E **58**, 6073 (1998).
[8] P. N. Segrè, S. P. Meeker, P. N. Pusey, and W. C. K. Poon, Phys. Rev. Lett. **75**, 958 (1995); **77**, 585 (1996).
[9] G. Brambilla, D. El Masri, M. Pierno, L. Berthier, L. Cipelletti, G. Petekidis, and A. B. Schofield, Phys. Rev. Lett. **102**, 085703 (2009).
[10] D. El Masri, G. Brambilla, M. Pierno, G. Petekidis, A. B. Schofield, L. Berthier, and L. Cipelletti, J. Stat. Mech. Theory Exp. (2009) P07015.
[11] G. Parisi and F. Zamponi, J. Chem. Phys. **123**, 144501 (2005).
[12] K. S. Schweizer, J. Chem. Phys. **127**, 164506 (2007).
[13] K. Kim and S. Saito, Phys. Rev. E **79**, 060501(R) (2009).
[14] M. Hermes and M. Dijkstra, J. Phys. Condens. Matter **22**, 104114 (2010).
[15] R. Juárez-Maldonado, M. A. Chavez-Rojo, P. E. Ramirez-Gonzalez, L. Yeomans-Reyna, and M. Medina-Noyola, Phys. Rev. E **76**, 062502 (2007).
[16] L. López-Flores *et al.*, e-print arXiv:1106.2475v1 [cond-mat.soft].
[17] D. A. McQuarrie, *Statistical Mechanics* (Harper and Row, New York, 1975).
[18] S. Chapman and T. G. Cowling, *The Mathematical Theory of Nonuniform Gases*, 2nd ed. (Cambridge University Press, Cambridge, 1952).
[19] M. Medina-Noyola, Phys. Rev. Lett. **60**, 2705 (1988).
[20] P. Mazur and U. Geigenmüller, Phys. A **146**, 657 (1987).
[21] P. E. Ramírez-González and M. Medina-Noyola, Phys. Rev. E **82**, 061503 (2010); **82**, 061504 (2010).